Atmospheric Environment 325 (2024) 120437

Contents lists available at ScienceDirect

Atmospheric Environment

journal homepage: www.elsevier.com/locate/atmosenv

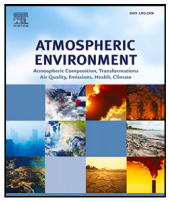

Modelled sources of airborne microplastics collected at a remote Southern Hemisphere site

Alex Aves [a,*], Helena Ruffell [a], Nikolaos Evangeliou [b], Sally Gaw [a], Laura E. Revell [a]

[a] School of Physical and Chemical Sciences, University of Canterbury, Christchurch, New Zealand
[b] Norwegian Institute for Air Research (NILU), Department of Atmospheric and Climate Research (ATMOS), Kjeller, Norway

HIGHLIGHTS

- Microplastics collected in atmospheric fallout at a remote New Zealand site.
- Daily microplastic deposition fluxes (150 MP m^{-2} day^{-1}) are on average 6× higher than weekly deposition fluxes (26 MP m^{-2} day^{-1}).
- Dispersion modelling reveals source regions from remote, terrestrial and oceanic regions.

ARTICLE INFO

Keywords:
Airborne microplastics
Remote
Deposition collection
Deposition fluxes
Sampling frequency
New Zealand
Micro-FTIR

ABSTRACT

Airborne microplastics have emerged in recent years as ubiquitous atmospheric pollutants. However, data from the Southern Hemisphere, and remote regions in particular, are sparse. Here, we report airborne microplastic deposition fluxes measured during a five-week sampling campaign at a remote site in the foothills of the Southern Alps of New Zealand. Samples were collected over 24-hour periods for the first week and for 7-day periods thereafter. On average, atmospheric microplastic (MP) deposition fluxes were six times larger during the 24-hour sampling periods (150 MP m^{-2} day^{-1}) than during the 7-day sampling periods (26 MP m^{-2} day^{-1}), highlighting the importance of sampling frequency and deposition collector design to limit particle resuspension. Previous studies, many of which used weekly sampling frequencies or longer, may have substantially underestimated atmospheric microplastic deposition fluxes, depending on the study design. To identify likely sources of deposited microplastics, we performed simulations with a global dispersion model coupled with an emissions inventory of airborne microplastics. Modelled deposition fluxes are in good agreement with observations, highlighting the potential for this method in tracing sources of deposited microplastics globally. Modelling indicates that sea-spray was the dominant source when microplastics underwent long-range atmospheric transport, with a small contribution from road dust.

1. Introduction

Microplastics (plastic debris 1–5000 μm in size) and nanoplastics (<1 μm) are near-ubiquitous atmospheric pollutants (Beaurepaire et al., 2021; Allen et al., 2022). Due to their small size and relatively low density, they are easily transported by wind (Bullard et al., 2021) and thus atmospheric transport is a major pathway for microplastics (MP) to reach remote regions (Evangeliou et al., 2020; Brahney et al., 2021). Microplastics are hazardous to marine and terrestrial ecosystems (de Souza Machado et al., 2018; Andrady, 2011) and can be harmful to human health through their introduction of toxic organic pollutants and potential interference with biological processes (Goodman et al., 2021; Prata, 2018).

Little is known about airborne microplastics in remote terrestrial areas of the Southern Hemisphere outside of a few studies carried out in Antarctica (Aves et al., 2022; Marina-Montes et al., 2022; González-Pleiter et al., 2021; Chen et al., 2023). Measurements from remote regions of the world are important to provide the background abundances needed to constrain the climate impacts of airborne microplastics (Revell et al., 2021), and as a benchmark to understand how environmental microplastic burdens are influenced by future potential policy actions (Allen et al., 2022).

Airborne microplastics are typically collected via passive collection or active sampling (Chen et al., 2020). These differing collection techniques mean comparisons between studies are difficult as standardized sampling protocols currently do not exist. Even with individual sampling techniques large variations exist. For example, deposition studies may use an automatic wet deposition sampler, or a simple open

* Corresponding author.
E-mail address: alexandra.aves@pg.canterbury.ac.nz (A. Aves).

https://doi.org/10.1016/j.atmosenv.2024.120437
Received 21 April 2023; Received in revised form 6 February 2024; Accepted 27 February 2024
Available online 1 March 2024

beaker or funnel over a bottle to collect total atmospheric fallout (Allen et al., 2019; Brahney et al., 2020; Knobloch et al., 2021). Knobloch et al. (2021) tested the impact of deposition sampler design on the abundance of microplastics collected, finding that a funnel over a bottle and an open beaker were similarly effective; while the funnel likely prevents sample re-suspension, it also may prevent particles from being collected in the first place. The duration of sampling may also play a role, with current studies being undertaken over days, weeks and months (summarized by Allen et al. (2022) and studies therein).

To assess the presence of airborne microplastics at a remote New Zealand site and test the influence of sampling frequencies, we collected airborne microplastics across both daily (24-h) and weekly (7-day) sampling periods (see Methods). The study was carried out in the foothills of the Kā Tiritiri o te Moana | Southern Alps of New Zealand; the first remote site used in an airborne microplastics study in New Zealand to date. To assess long-range transport of the microplastics deposited at the study site, we use a Lagrangian model, which we combine with recently published global emission inventories for microplastics (Evangeliou et al., 2022). This provides a modelled source contribution analysis to the measured deposition rates giving a novel insight into their origin.

2. Materials and methods

2.1. Field sampling

Sampling was carried out at the University of Canterbury's Mt John Observatory in the Mackenzie district (43.9853°S, 170.4641°E, 1031 m above sea level, Fig. S1). Ōtehīwai | Mt John is situated in the foothills of the Southern Alps on the eastern side, and approximately 80 km from either coast. The Mackenzie district is largely unpopulated: the nearest town Tekapo has a population of 550, with the total population of the entire Mackenzie district 4866 over an area of 7139 km^2 (Statistics New Zealand, 2018), which equates to 1 person per 1.42 km^2.

Two sampling periods were completed to collect both daily and weekly deposition data. In the first sampling period, samples were collected in triplicate every 24 h for 7 days (21 samples total), hereafter 24-h samples. In the second sampling period, samples were collected in triplicate every 7 days for four weeks (12 samples total), hereafter 7-day samples. These sampling periods were selected to investigate whether sampling frequency significantly influences the number of microplastics collected. For both sampling periods, three 1 L glass sampling vessels with a surface area of 0.006 m^2 (mouth diameter of 0.09 m) were placed in a purpose-built stainless-steel holder (Fig. S24) and the lids were removed. After the sampling period, the collectors were sealed with their lids at the site and replaced with new, pre-cleaned sampling collectors for the next sampling period. The collection and set-up of this study followed methods previously reported in the literature (Table. S9), which presents deposition sampling as an accessible option for passive microplastic collection.

Weather data was taken from a nearby weather station (Table. S4 and Table. S8) which sits at an elevation of 762 m a.s.l. Over the daily sampling periods there was no precipitation recorded, temperature averaged 3.3 °C across the daily sampling periods and the wind came from a predominantly North to North-West direction with a 3 m s^{-1} average wind speed. Over the weekly sampling periods, week 1 received 13.9 mm of precipitation, week 2, 2.1 mm, week 3, 0 mm and week 4, 2.5 mm. Average temperature across the four weeks was 3.7 °C, with week 1 averaging under 0 °C. Wind direction was mostly SW–NW, with wind speeds averaging 2.7 m s^{-1}.

2.2. Laboratory analysis

Each sample collector was rinsed with 100–200 mL of ultra-pure water to ensure re-suspension of any particles present. The contents of the sample were vacuum filtered onto a glass microfibre filter (Whatman GF/C; 1.2 μm pore size; 47 mm diameter). All glassware was flushed five times with approximately 100–200 mL of ultra-pure water to ensure all sample contents were removed. The sample was then vacuum filtered, rinsing all sides of the filter apparatus three times with ultra-pure water and once with 70% ethanol after filtration. The filtering apparatus opening was covered in aluminium foil during the filtering process. Once dry, the filter was removed with stainless steel tweezers and placed in a petri dish ready for visual analysis.

2.3. μFTIR identification of microplastics

Filter papers were analysed using a Leica MZ125 stereomicroscope (10× magnification) for visual identification of microplastics. Visual identification was based on previously identified characteristics of microplastics related to type, shape, degradation, colour and physical characteristics, as well as equal thickness of fibres, lack of cellular structure, and homogeneous colour (Chen et al., 2020). Four main morphotypes were used to categorize microplastics: films, fibres, fragments and beads. Colours were also recorded for each suspected microplastic particle.

Following visual identification, all suspected microplastics were chemically analysed using micro-Fourier Transform Infrared Spectroscopy (μFTIR) as described by Aves et al. (2022). Between 0%–50% of chemically analysed particles were confirmed as plastic polymers in each sample (Table. S2 and Table. S6). Using pre-existing methods for image analysis of microplastic characterization (Primpke et al., 2018), a Hyperion 2000 microscope (Bruker Optics) attached to a Vertex 70 (Bruker Optics) spectrometer, mercury cadmium detector (MCD) super-cooled with liquid nitrogen, was used for polymer identification. Suspected polymers were manually placed onto a calcium fluoride disk (CaF_2; 6 mm) using tweezers and a drop of 96% ethanol (to aid in transfer). An overview image was taken before infra-red measurements were performed at 15× magnification. Scans were run in transmission mode (10 scans, 4 cm^{-1} resolution, spectral range of 4000–1000 cm^{-1}) using OPUS 7.8 software. A Wiley spectral library was used to run all spectra against (databases: industrial chemicals, pure organic compounds; organosilicons; polymers, Hummel defined basic; Sadtler acrylates and methacrylates; Sadtler fibres and textile chemicals; Sadtler fibres by microscope; Sadtler inorganics; Sadtler polymers and monomers (comprehensive); Sadtler polymers, Hummel; Sadtler standards (organic and polymeric compounds subset); Sigma-Aldrich library of FTIR spectra). Particles returning a hit quality index (HQI) of >70% were accepted as microplastics and anything less that displayed characteristic plastic peaks was compared against library reference spectra to confirm identification.

2.4. Modelling

To track the transport and origin of the deposited atmospheric microplastics, the Lagrangian particle dispersion model FLEXPART version 10.4 was used (Pisso et al., 2019). The model was driven with hourly ERA5 assimilated meteorological analyses (Hersbach et al., 2020) retrieved from the European Centre for Medium-Range Weather Forecasts (ECMWF) consisting of 137 vertical levels and a horizontal resolution of 0.5° × 0.5°. The emission sensitivities were calculated in backwards time (retroplume) mode, using a new feature of FLEXPART that reconstructs wet and dry deposition with backward simulations (Eckhardt et al., 2017).

Wet deposition of microplastics was reconstructed after releasing computational particles at Mt John Observatory (receptor) at altitudes of 0–20 km above sea level, as scavenging occurs at any height of the

atmosphere, depending on the location of clouds. For dry deposition, particles were released at 0–30 m at the same receptor, as this shallow layer is equal to the height of the layer in which, in forward mode, particles are subject to dry deposition. All released particles represent a unity deposition amount, which was converted immediately (i.e. upon release of a particle) to atmospheric concentrations using the deposition intensity as characterized by either the dry deposition velocity or wet scavenging rate (in-cloud and below-cloud scavenging; Eckhardt et al. (2017) and Grythe et al. (2017)). This gives the sensitivities between emissions and deposition amounts (30-day backward tracking).

The model output consists of a spatially gridded sensitivity of microplastic deposition (wet and dry) at the receptor point to the respective emissions, equivalent to the backwards time mode output for concentrations (Seibert and Frank, 2004). Deposition rates of microplastics (in particles m^{-2} day^{-1}) can be computed by multiplying the emission sensitivities (in m) divided by the lowest model layer (100 m) with gridded emissions (in MP m^{-2} day^{-1}). In the present study, we used global emissions for microplastics and microfibres from Evangeliou et al. (2022) calculated with inverse modelling. Five sources for atmospheric microplastics were considered, namely (i) ejection from the surface of the ocean due to wave breaking and bubble bursting, (ii) from the agricultural sector (e.g., loss from agricultural nets), (iii) from mineral dust (e.g., previously deposited microplastics in desert regions remobilised with dust), (iv) from road dust of freight and passenger automobiles (e.g., tyre and brake wear), and (v) microfibres from clothes (population-constrained emissions). This provides a modelled source contribution analysis to the measured deposition rates giving a novel insight into their origin.

2.5. Quality control

The collection jars used were glass with the holder used for the collectors made entirely out of stainless steel. Placement and changeover of collectors were always undertaken standing downwind of the samplers. When sample collectors were placed in the field, natural fibre clothing was worn and fieldwork was completed by the same two people over the sampling period. Lids were removed, wrapped in foil and stored inside a cardboard box during the sampling periods. The site chosen was located on private land, next to a private accommodation site for researchers. This site had limited access over the duration of sampling.

Two laboratory blanks were made up of 500 mL of ultra-pure water (<18 MΩ) in the glass sampling collectors and were refrigerated for the sampling duration. Storing for the duration of sampling was done to mimic the field samples which were also being stored for the same length of time and in the same way before being processed for analysis. Samples were refrigerated prior to analysis to prevent growth of any biological material that may have been collected. These then underwent identical laboratory analysis as field samples to identify any contamination from the sampling collectors. Daily blanks were processed alongside the field sample analysis to ensure any contamination was identified throughout the laboratory process. These samples were processed following identical methodologies of field samples, with the sample made up of approximately 500 mL of ultra-pure water.

All equipment was rinsed thoroughly before use. Sample collectors were washed with Decon90 detergent and soaked for 24 h before they were rinsed three times with ultrapure water and once with acetone, and left covered in aluminium foil to dry in a fume hood. Plastic use was minimized throughout the whole sampling and extraction process to ensure contamination levels from sampling were as low as possible.

The glass collectors used for sampling had an orange seal that sits between the lid and the body of the vessel. Spectroscopic analysis of the seal was undertaken to ensure contamination was accounted for.

2.6. Blank corrections

Spectroscopic analysis of orange and pink fragments identified in both the laboratory blanks and in field samples confirmed them to be alkyd and silicone particles. These particles were excluded from further analysis and the results. Daily laboratory blanks contained zero plastic particles so no further corrections were made to the results.

3. Results

3.1. Microplastic characteristics

Characteristics of airborne microplastics collected in the 24-h samples and 7-day samples are shown in Figs. 1 and 2, respectively. There were a total of 12 types of plastic polymers identified, with polyethylene terephthalate (PET) being the most common (29%). Fibres were the most common morphotype (65%), followed by fragments (32%), with a single bead present during weekly sampling. Blue was the most common colour identified (47%). Microplastic sizes ranged from 50–3550 μm, with 74% of particles <600 μm and the smallest identified particle 52 μm, which was limited by the analysis technique used of manual μFTIR.

3.2. Deposition fluxes

24-h deposition fluxes averaged 150 ± 25 (SE) MP m^{-2} day^{-1} (Fig. 3), while the 7-day deposition fluxes were significantly smaller, averaging 26 ± 8 (SE) MP m^{-2} day^{-1} (Fig. 3). The closest previous study to the measurement site was carried out in Christchurch, approximately 200 km to the north-east of this study site (Knobloch et al., 2021). Knobloch et al. (2021) used 6-day sampling periods and identified deposition rates of 19–47 MP m^{-2} day^{-1}, which is similar to those for the 7-day sampling periods reported here. Table 1 provides a comparison of deposition fluxes, sampling frequencies and analysis methods from previous studies.

3.3. Modelling microplastic transport and sources

Modelled deposition of microplastics ranged from 4.5–48 MP m^{-2} day^{-1} for the daily samples (Fig. 4). Since the emissions inventory assumes that fibres correlate with population and do not undergo long-range transport (Evangeliou et al., 2022), we compare modelled (fragment) deposition fluxes with measured fragment deposition fluxes, and find good agreement between the two. The 7-day modelled deposition rates are between 4.3–35 MP m^{-2} day^{-1}. 24-h modelled deposition fluxes show closer agreement with observations than the 7-day modelled deposition fluxes as the modelled meteorology is more accurate. This further highlights the advantage of daily deposition sampling when combining observations with modelling to identify source contributions.

Several particle sizes were simulated to track the origin and sources of atmospheric microplastics deposited at the Mt John Observatory measurement site. The resulting footprint emissions sensitivities for the wet and dry deposited mass can be seen in Fig. 5. During the daily sampling periods, atmospheric microplastics originated from the north-west, west and south-west, consistent with prevailing winds at Mt John Observatory and the nearby township of Tekapo (Macara, 2016).

During days 2–4 of sampling, atmospheric-transported microplastics that were collected at Mt John Observatory originated from the south. The air shifted in days 5–7, coming from the west. Modelling indicates that atmospheric microplastics may have originated from the Australian coasts, which are approximately 2000 km away (Fig. 6). For the 7-day samples, the average footprint emission sensitivities showed multi-directional origin of the deposited microplastics. Dry deposition dominated and was responsible for >70% of the mass deposited at the receptor site.

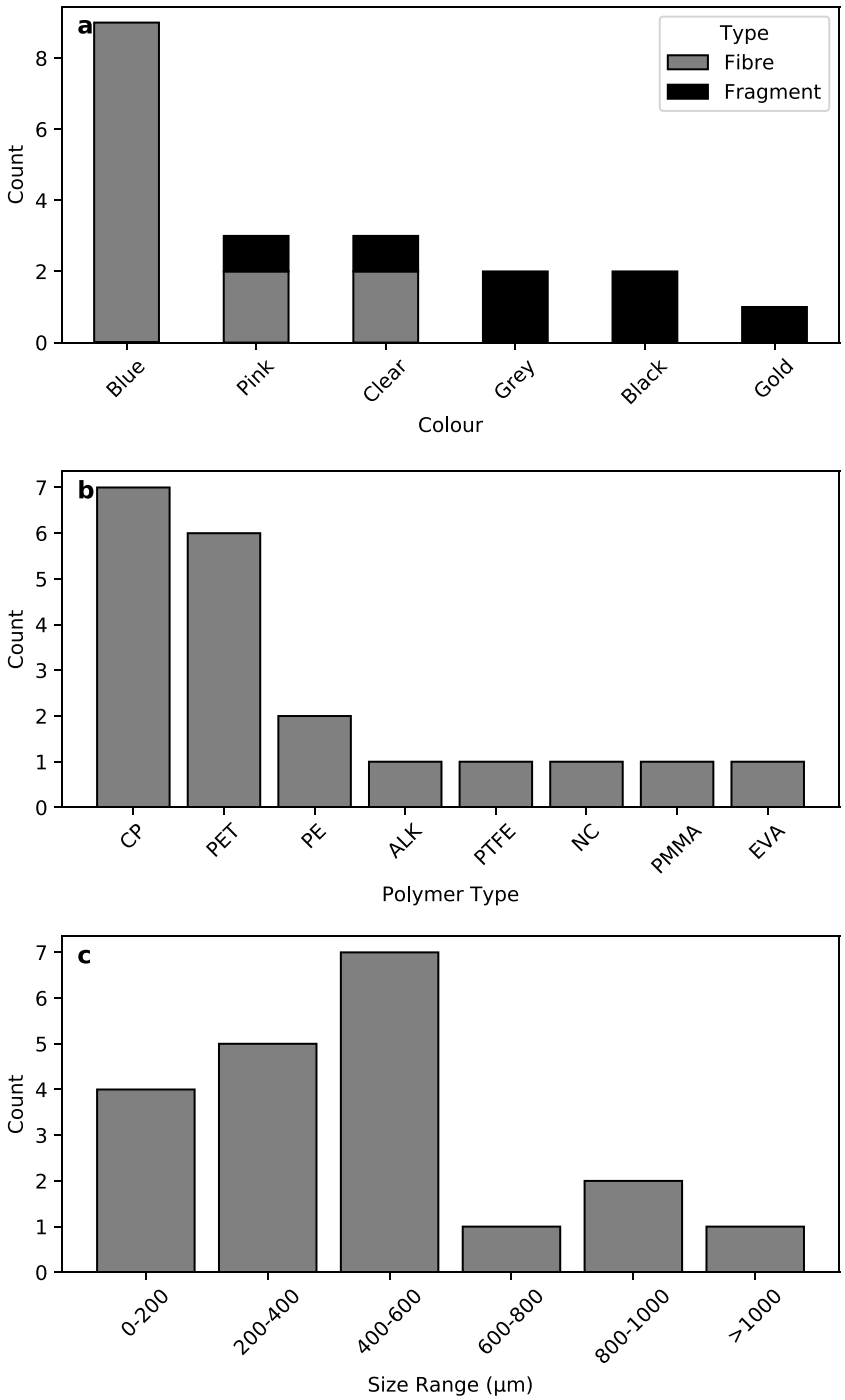

Fig. 1. Characteristic data of microplastics collected during daily sampling periods. (a) Count of MP's split by colour and morphotype; (b) count of MP's grouped by polymer type; (c) count of MP's grouped by size.

Global dispersion models like FLEXPART are suitable to investigate sources that are resolved by the meteorological fields used. In the present case, the transport can be resolved in a 0.5° × 0.5° resolution grid. While this is sufficient for the map domain of Fig. 6, it cannot track the terrestrial contribution from New Zealand as it is a small country with complex terrain.

To investigate whether local sources could contribute to the findings at the receptor, the mesoscale model, FLEXPART-WRF version 3.3.2 was used (Brioude et al., 2013). The model is based on the same principles as FLEXPART and is not described here to avoid repetition. However, one feature that has not been implemented yet is wet and dry deposition backwards such as in the standard FLEXPART (Eckhardt et al., 2017). This means it cannot calculate deposited concentrations, but it can only give an indication of the origin of the air at the surface of the receptor (Mt John Observatory). Here, we use a version specifically designed to model microplastics with respect to measured density and wet removal. The respective footprint emissions sensitivities in 12 and 3 km resolution are depicted in Supplementary Figures S1–S11. The footprints, although they correspond to surface air and not deposited mass, correlate very well with those from the main FLEXPART simulations shown in Fig. 6. They all agree that transport of air to Mt John Observatory was predominantly coming from a south-westerly direction or from the ocean and never from the populated cities of the north (Auckland and Wellington) or east (Christchurch).

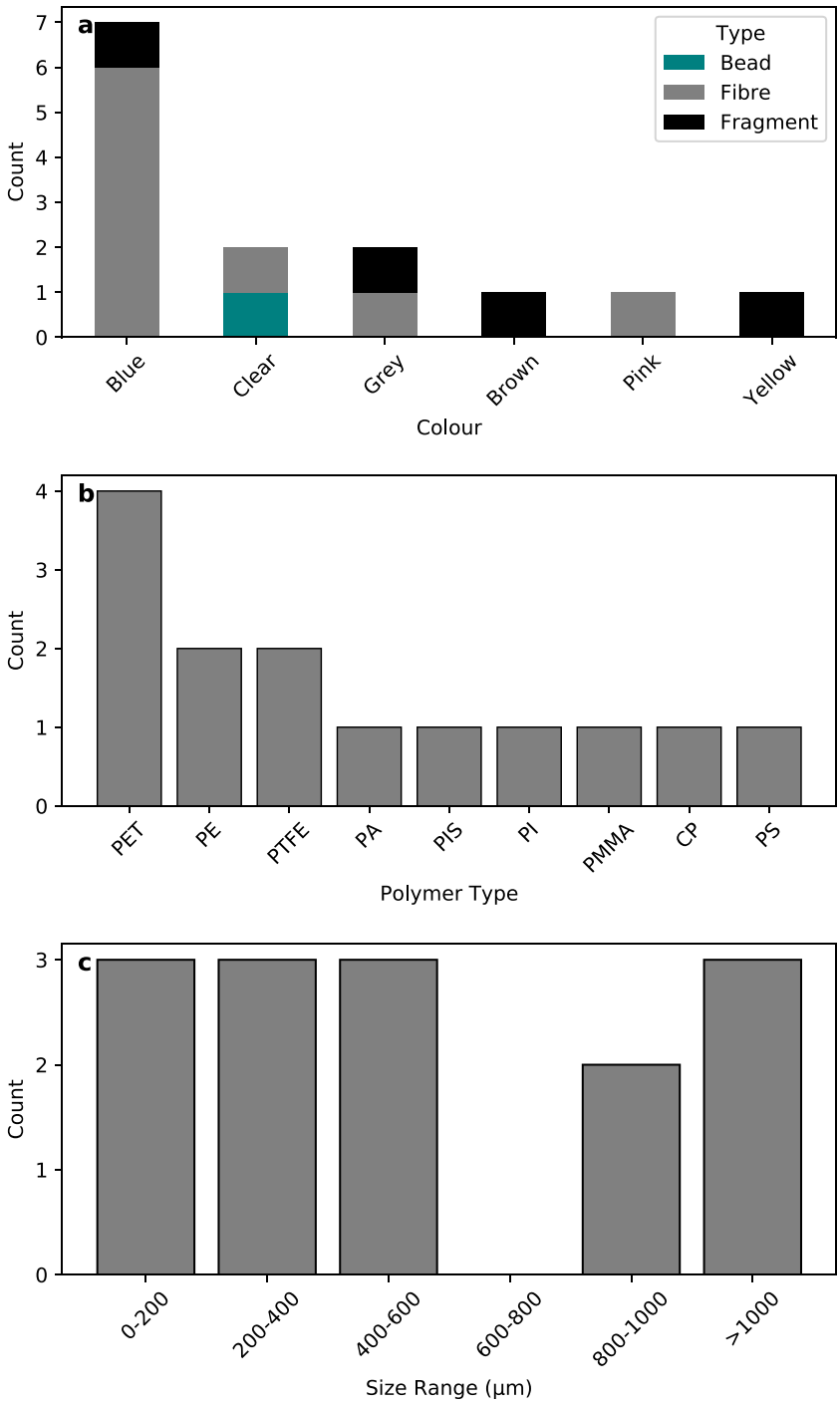

Fig. 2. Characteristic data of microplastics collected during weekly sampling periods. (a) Count of MP's split by colour and morphotype; (b) count of MP's grouped by polymer type; (c) count of MP's grouped by size.

4. Discussion

This study identified the presence of airborne microplastics at a remote site in New Zealand, with deposition rates comparable to those reported at urban sites around the world (Table 1). The study site was situated at 1031 m above sea level in a district with a very low population density. This region is usually dominated by tourism, however the New Zealand border was closed to international visitors at the time sampling was carried out due to the pandemic restriction measures. The deposition fluxes reported highlight the ubiquitous nature of airborne microplastics even in sparsely populated regions (Table 1).

The contribution of airborne microplastics originating outside of New Zealand is a possibility. Mineral dust has a reported density of 2.65 g cm^{-3} (Osborne et al., 2008) compared to microplastics which range from 0.85–1.41 g cm^{-3} (Morét-Ferguson et al., 2010), identifying the potential for plastics to remain airborne for long periods of time and be transported over large distances. Dust originating from Australia can be transported 3000 km over open ocean to the West Coast of New Zealand before being deposited in the Southern Alps (McGowan et al., 2005). The Australian bush-fires in 2019–2020 left West Coast glaciers in New Zealand covered in layers of smoke, ash and dust which has the potential to influence albedo in the region (Yasunari et al., 2011). With the addition of deposited microplastics in an assortment of colours and

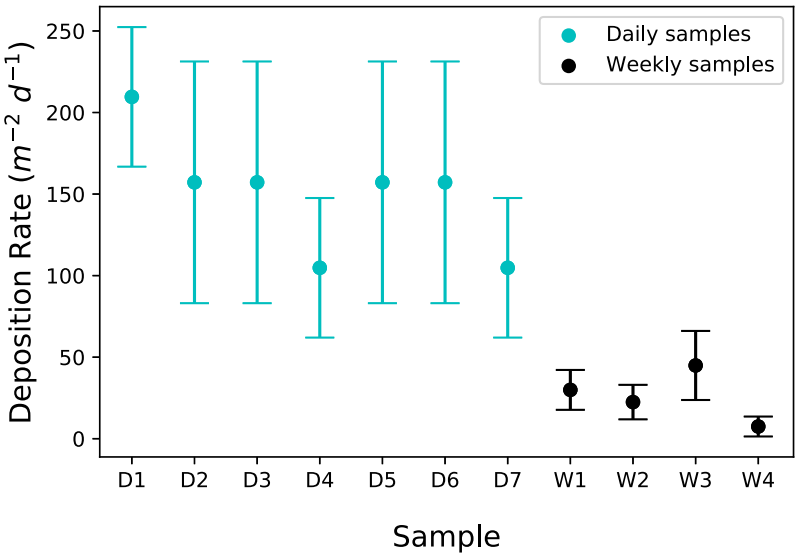

Fig. 3. Measured deposition rates of microplastics at the remote station. Daily and weekly sample means ±SE.

Table 1
Deposition fluxes reported by previous studies in ascending order of average deposition flux.

Location	Sampling frequency	Deposition flux (MP m^{-2} day^{-1})[a]	Analysis technique
Nottingham, United Kingdom (Stanton et al., 2019)	2 weeks	2.9	Visual; μFTIR
Kassel, Central Germany (Kernchen et al., 2022b)	Monthly	10 (wet); 5 (dry) (0–23)	Visual; μFTIR; μRaman
Gdynia, Poland (Szewc et al., 2021)	1–8 days	10 (0–30)	Visual; μATR FTIR
Ireland (Roblin et al., 2020)	24 h	12 (10–15) (fibres)	Visual; hot needle; μRaman
Shiraz, Iran (Abbasi and Turner, 2021)	Monthly	64 (27–116) (City); 12 (6–19) (Remote)	Visual; μRaman
Ancol, North Jakarta, Indonesia (Purwiyanto et al., 2022)	Monthly	15 (3–40)	Visual; μFTIR
Christchurch, New Zealand (Knobloch et al., 2021)	6 days	19–47	Visual; μFTIR
Mackenzie District, New Zealand (This study)	Weekly	26 (0–90)	Visual; μFTIR
Paris, France (Dris et al., 2016)	Various frequencies	110 (urban); 53 (suburban) (2–355)	Visual; μFTIR
Guangzhou, China (Yuan et al., 2023)	Monthly	66 (21–109)	Visual; μFTIR
Ho Chi Minh City, Vietnam (Strady et al., 2021)	3–4 days	71–917	Visual; μFTIR
Weser River catchment, Germany (Kernchen et al., 2022a)	Monthly	99 (10–367)	μFTIR
Guangzhou, China (Huang et al., 2021)	22–40 days	114 (51–178)	Visual; μFTIR
Sao Paulo, Brazil (Amato-Lourenço et al., 2022)	15 days	123 (4–203)	Nile red; FTIR-ATR
North American wilderness areas (Brahney et al., 2020)	Weekly, bi-weekly, monthly	132 (48–435)	Visual; μFTIR
Mackenzie District, New Zealand (This study)	Daily	150 (0–314)	Visual; μFTIR
Dongguan, China (Cai et al., 2017)	30–31 days	228 (175–313)	Visual; μFTIR
Hamburg, Germany (Klein and Fischer, 2019)	Bi-weekly	275 (136–512)	Nile red; μRaman
New Jersey, USA (Yao et al., 2022)	14 days	327	Visual; SEM; μRaman
Lanzhou, China (Liu et al., 2022)	1–14 days	354 (57–689)	Visual; μFTIR
Pyrenees Mountains, France (Allen et al., 2019)	Monthly	365 (204–599)	Visual; Nile red; μRaman
London, United Kingdom (Wright et al., 2020)	3.5 days	771 (575–1008)	Nile red; μFTIR
Qaqulluit National Wildlife Area, Nunavut, Canada (Hamilton et al., 2021)	24–48 h periods	2433	Visual; μFTIR; μRaman
Shanghai, China (Jia et al., 2022)	Daily	3261	Visual; μFTIR
Auckland, New Zealand (Fan et al., 2022)	Weekly	5955 (73–19,476) (urban); 3349 (582–12,159) (suburban)	Nile red; Py-GC/MS
Quzhou County, North China Plain (Li et al., 2023)	Individual rainfall event	7125 (79–74,808)	Nile red; μFTIR
Shiraz, Iran (Abbasi, 2021)	10 min	12,672 (2880–22,608)	SEM-EDX; μRaman

[a] The average deposition flux is reported with the range in brackets.

morphotypes, these pollutants may then also play a role in influencing the Earth's radiative balance (Evangeliou et al., 2020; Revell et al., 2021).

Here, we used emissions from Evangeliou et al. (2022) to calculate modelled deposition fluxes that compare fairly well to those observed, given the large uncertainties associated with current emissions. Some of the agreement likely originates from the fact that the same analysis technique used here, μFTIR spectroscopy, was also used to analyse the samples from which the emissions inventory is derived (Brahney et al., 2020). As shown here, Lagrangian modelling enables the origin of the deposition fluxes to be mapped to identify what sectors contribute the most and also to identify which regions are responsible for the deposited microplastic fluxes.

Fig. 4 depicts the percentage that every sector contributes to the modelled deposition fluxes. In all cases, both for 24-h and 7-day samples, the deposited microplastics were mostly emitted from the ocean, with a smaller portion from road dust due to transport on roads in New Zealand, but also in Australia. The other sectors had a diminutive contribution. Fibres have previously been shown to correlate with population (Brahney et al., 2021). Although detected in the samples (Figs. 1 and 2), they are not projected to be transported from nearby sources due to the low population density of the area (1 person per 1.42 km^2) and prevailing wind direction: the nearest town is east of the

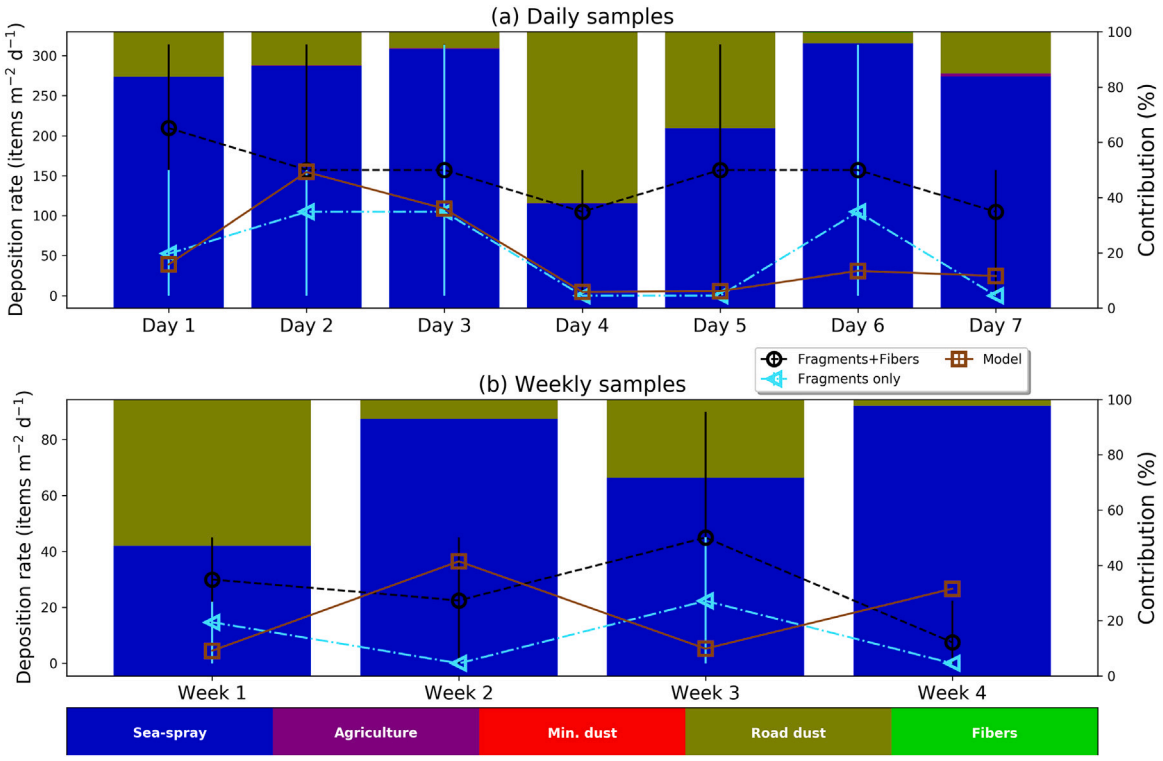

Fig. 4. Measured and modelled deposition rates of microplastics at the remote station. Observation minimum, maximum and mean values from the triplicate sampling are shown as circles for all microplastics (fragments and fibres) and as triangles for fragments only. Modelled deposition rates are shown as squares. (a) 24-h samples; (b) 7-day samples. Microplastics originated from sea-spray and road dust sources, as indicated by the coloured shading.

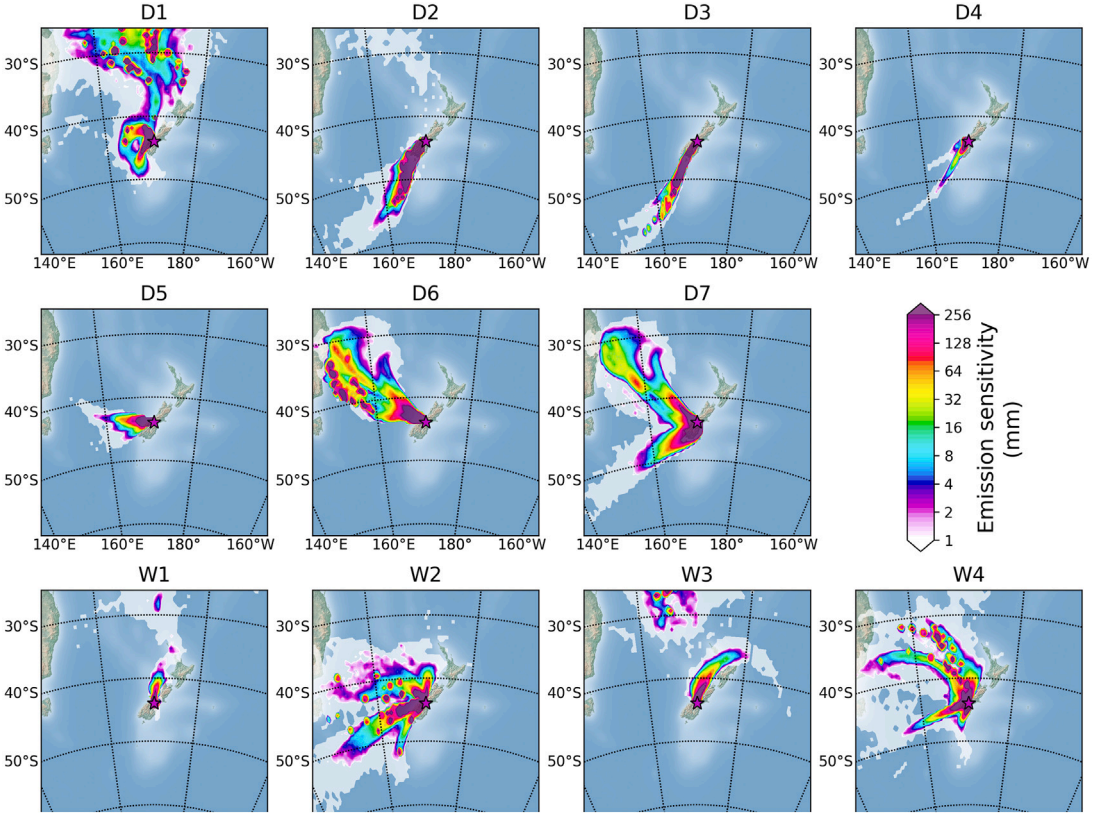

Fig. 5. Footprint emissions sensitivities for dry and wet deposited mass using the FLEXPART retroplume mode developed by Eckhardt et al. (2017). The emission sensitivity expresses the probability of any release occurring in each grid cell to reach the receptor (Mt John Observatory).

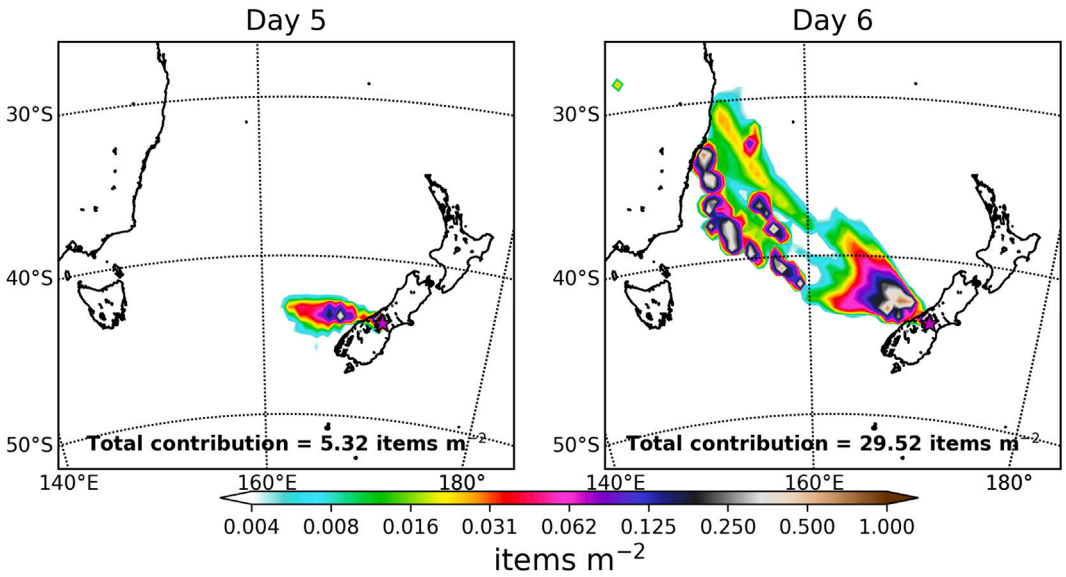

Fig. 6. Source contribution to modelled microplastic deposition rates on days 5 and 6 in FLEXPART simulations with 0.5° × 0.5° resolution. Five sources of microplastics were considered, namely from sea-spray, agricultural activity, mineral and road dust and fibres.

study site, while winds originated predominantly from the northwest to southwest during the study period. Yang et al. (2022) found from tank experiments that fibres are not co-emitted with sea-spray aerosol due to their large size and density. Hence, the presence of fibres in the measured samples might be (i) due to the resuspension of fibres previously transported and deposited at remote sites of New Zealand from populated areas (e.g. the North Island or the East coast of the South Island) or (ii) due to actual resuspension from the ocean with wave breaking and bubble bursting. Note that the emissions of microfibres used here to calculate modelled deposition fluxes for microfibres (Evangeliou et al., 2022) were obtained assuming they only correlate with population and, thus, they are not emitted from the surface of the ocean.

The regions that contributed to deposited microplastics at Mt John Observatory are mapped in Fig. S13–S23. In almost all cases, the regions contributing to the modelled fluxes are oceanic domains south or west of New Zealand. To show how long-range transported microplastics could affect even this remote site, we focus on samples taken on days 5 and 6 (Fig. 6). During these two days, the air was coming from the northwest, mainly from the ocean, but extending to the Australian coasts (Fig. 5). However, road dust was also transported from the Australian coast and deposited in Mt. John Observatory. Although the portion of the deposited road dust is rather small, it proves that even large-size microplastics can be transported from very far distances and deposited in remote sites.

The total microplastic deposition fluxes recorded over the four 7-day sampling periods were on average 6× less than the number of microplastics collected over the total 24-h sampling periods. This difference may be due to the longer time frame which allows for the re-suspension of particles to leave the collectors, compared to 24-h samples which are capped after a shorter period, highlighting the importance of sampling duration and design. Table S9 presents the differing collection types used throughout past studies as well as sampling duration. Studies with the shortest sampling frequencies of 10 min and 1 rainfall event, presented the highest average deposition fluxes of 12,672 MP/m^{-2}/d^{-1} and 7125 MP/m^{-2}/d^{-1}, respectively (Abbasi, 2021; Li et al., 2023), whilst deposition rates decreased for studies of increased duration (Table 1).

To investigate this, further sampling needs to be undertaken across different time periods to determine if re-suspension was the leading cause for lower rates over a longer sampling period. Different sampling techniques and sampler designs also need to be considered, and the pairing of both passive and active sampling methods would permit further understanding of the extent of this problem (Zhang et al., 2020). Therefore, we recommend completing multiple sampling periods of differing durations for passive airborne microplastic studies to gain a deeper understanding of the impact of resuspension on deposition sampling studies. It is also recommended that future airborne microplastic field studies should include field blanks which are exposed to the sampling site for a short period (i.e. 30 s) and handled in the same way as field samples to account for any contamination from sample handling.

Future work will explore simultaneous sample collection over differing durations to further understand the impact this has on microplastic deposition study findings. Studies completed using daily sampling frequency over longer time periods would allow us to explore seasonal trends and couple findings with weather data and sampling techniques more accurately. These findings draw attention to the many variables within airborne microplastic research, starting from the sampling frequency of the study, the collection type used and the analysis technique performed for microplastic identification.

Previous studies in Antarctica, the Pyrenees and the USA have all identified PET in deposition studies in remote areas (Aves et al., 2022; Allen et al., 2019; Brahney et al., 2020). PET represents over 50% of synthetic fibres produced globally (Sinha et al., 2010), highlighting the textile industry as a dominant source for airborne microplastic pollution. This study aligns with previous findings (Aves et al., 2022; Liu et al., 2019; Dris et al., 2016; Bullard et al., 2021; Cai et al., 2017; Knobloch et al., 2021) which also identified fibres as the most common morphotype in airborne studies compared to previous findings from European studies which found higher levels of fragments (Allen et al., 2019; Klein and Fischer, 2019). There were no obvious patterns for microplastic characteristics across the samples collected (Figs. 1 and 2), likely because the number of microplastics identified in the study was small. Furthermore, given the analysis techniques used, sizes reported are limited to >52 μm.

The chemical analysis technique used in this study, manual μ-FTIR, is limited in its ability to report particles <52 μm, in this study, which limits the understanding of smaller microplastic particles (1 μm–50 μm). Most studies to date have explored the long-range transport of microplastics assuming spherical properties, yet fibres are generally the most abundant morphotype (Mbachu et al., 2020). Recent work has pointed to a change in the settling velocity and differences in long-range transport capabilities compared to previously explored spherical

particles (Xiao et al., 2023). As fibres made up the largest proportion of morphotypes in our study, it is evident that fibrous microplastics are being moved through the atmosphere to these remote locations, with recent research highlighting the specific characteristics of fibres make them more susceptible to longer vertical and horizontal airborne transport compared to spherical particles (Tatsii et al., 2023). The analysis technique used limits the size of reported particles, yet previous literature shows the size distribution skewed to sub 10 μm particles (Levermore et al., 2020). Based on this assumption, modelling results presented are exploratory.

Deposition collection is an accessible, affordable and effective sampling technique for airborne microplastic research. For more in depth understanding, the pairing of both passive air sampling and active air sampling methods would be beneficial. This study highlights that changing just one variable – sampling frequency – can yield major impacts on reported results. This indicates that sampling frequency should be carefully considered in future atmospheric microplastic deposition studies. Further research is required to understand the scale of airborne microplastic pollution across other regions of New Zealand and the wider Southern Hemisphere. For future studies, the collection of long term, simultaneous data collection using varied sample collection techniques, sampling durations and analysis methodologies would be beneficial for the microplastic community. The microplastic deposition fluxes reported in this remote region were similar in magnitude to those recorded in urban Christchurch, suggesting the potential for airborne microplastics to be abundant across New Zealand, even in remote areas. Further research into the potential risks and impacts for human, aquatic and terrestrial organisms in New Zealand is required now that airborne microplastics have been identified in both urban and remote regions.

5. Conclusions

Deposition fluxes of atmospheric microplastics from this study of a remote site in New Zealand averaged 150 MP m^{-2} day^{-1} over 24-h collection periods and 26 MP m^{-2} day^{-1} over 7-day sampling periods. At present, these results report the first remote deposition fluxes of airborne microplastics in New Zealand. Samples collected over 24-h periods showed significantly larger microplastic deposition rates than samples collected over 7-day periods. Re-suspension of microplastic particles is likely to have occurred during the 7-day sample periods due to the extended length of sampling and the type of sample collector used. In response to these findings, we recommend that future deposition studies for airborne microplastic research prioritize daily sampling and consider all aspects of variation in sample collection, duration and analysis. Further research is needed to investigate how variable these results are across different seasons and at urban sites within New Zealand, as well as the influence of sampling duration as a variable in particle re-suspension. Through the use of a global dispersion model coupled with an emissions inventory of airborne microplastics, this research highlights the long-range transport which microplastics undergo through the atmosphere. Microplastics travelled over thousands of kilometres to reach the studied sampling site, with sources predominantly from sea-spray and road dust.

CRediT authorship contribution statement

Alex Aves: Conceptualization, Investigation, Methodology, Visualization, Writing – original draft, Writing – review & editing. **Helena Ruffell:** Methodology, Writing – review & editing. **Nikolaos Evangeliou:** Methodology, Software, Visualization, Writing – review & editing. **Sally Gaw:** Supervision, Writing – review & editing. **Laura E. Revell:** Conceptualization, Supervision, Writing – original draft, Writing – review & editing.

Declaration of competing interest

The authors declare that they have no known competing financial interests or personal relationships that could have appeared to influence the work reported in this paper.

Data availability

Data will be made available on request.

Acknowledgements

This research was supported by the Royal Society of New Zealand Marsden Fund, New Zealand (grant no. MFP-UOC1903). AA acknowledges support from the University of Canterbury Gateway Antarctica Ministry of Foreign Affairs and Trade Scholarship in Antarctic and Southern Ocean Studies and the University of Canterbury Aho Hīnātore Scholarship. LER appreciates support by the Rutherford Discovery Fellowships from New Zealand Government funding, administered by the Royal Society Te Apārangi. NE was funded by the Norwegian Research Council (NFR) project MAGIC (Airborne Microplastic Detection, Origin, Transport and Global Radiative Impact, Project No.: 334086). We acknowledge the help of Nigel Frost who supported the continuation of sampling at Mt John Observatory and Nick Oliver's design and production of the stainless steel sampling holder. We acknowledge both Paula Brooksby and Alex Nichols for the help provided with the use of the μFTIR. We acknowledge mana whenua Ngāi Tahu and Ngāi Tūāhuriri, on whose lands our sampling, analysis and writing took place.

This modelling analysis has used a virtual access service that is supported by the European Commission under the Horizon 2020 – Research and Innovation Framework Programme, H2020-383 INFRAIA-2020-1, ATMO-ACCESS Grant Agreement number: 101008004, while all simulations were performed on resources provided by Sigma2 — the National Infrastructure for High Performance Computing and Data Storage in Norway.

Appendix A. Supplementary data

Supplementary material related to this article can be found online at https://doi.org/10.1016/j.atmosenv.2024.120437.

References

Abbasi, S., 2021. Microplastics washout from the atmosphere during a monsoon rain event. J. Hazard. Mater. Adv. 4, 100035.

Abbasi, S., Turner, A., 2021. Dry and wet deposition of microplastics in a semi-arid region (Shiraz, Iran). Sci. Total Environ. 786, 147358.

Allen, D., Allen, S., Abbasi, S., Baker, A., Bergmann, M., Brahney, J., Butler, T., Duce, R.A., Eckhardt, S., Evangeliou, N., et al., 2022. Microplastics and nanoplastics in the marine-atmosphere environment. Nat. Rev. Earth Environ. 1–13.

Allen, S., Allen, D., Phoenix, V.R., Roux, G.L., Jiménez, P.D., Simonneau, A., Binet, S., Galop, D., 2019. Atmospheric transport and deposition of microplastics in a remote mountain catchment. Nat. Geosci. 12 (5), 339–344. http://dx.doi.org/10.1038/s41561-019-0335-5.

Amato-Lourenço, L.F., dos Santos Galvão, L., Wiebeck, H., Carvalho-Oliveira, R., Mauad, T., 2022. Atmospheric microplastic fallout in outdoor and indoor environments in Sao Paulo megacity. Sci. Total Environ. 821, 153450.

Andrady, A.L., 2011. Microplastics in the marine environment. Mar. Pollut. Bull. 62 (8), 1596–1605.

Aves, A.R., Revell, L.E., Gaw, S., Ruffell, H., Schuddeboom, A., Wotherspoon, N.E., LaRue, M., McDonald, A.J., 2022. First evidence of microplastics in Antarctic snow. Cryosphere 16 (6), 2127–2145.

Beaurepaire, M., Dris, R., Gasperi, J., Tassin, B., 2021. Microplastics in the atmospheric compartment: a comprehensive review on methods, results on their occurrence and determining factors. Curr. Opin. Food Sci. 41, 159–168.

Brahney, J., Hallerud, M., Heim, E., Hahnenberger, M., Sukumaran, S., 2020. Plastic rain in protected areas of the United States. Science 368 (6496), 1257–1260. http://dx.doi.org/10.1126/science.aaz5819.

Brahney, J., Mahowald, N., Prank, M., Cornwell, G., Klimont, Z., Matsui, H., Prather, K.A., 2021. Constraining the atmospheric limb of the plastic cycle. Proc. Natl. Acad. Sci. 118 (16), e2020719118. http://dx.doi.org/10.1073/pnas.2020719118.

Brioude, J., Arnold, D., Stohl, A., Cassiani, M., Morton, D., Seibert, P., Angevine, W., Evan, S., Dingwell, A., Fast, J.D., et al., 2013. The Lagrangian particle dispersion model FLEXPART-WRF version 3.1. Geosci. Model Dev. 6 (6), 1889–1904.

Bullard, J.E., Ockelford, A., O'Brien, P., Neuman, C.M., 2021. Preferential transport of microplastics by wind. Atmos. Environ. 245, 118038.

Cai, L., Wang, J., Peng, J., Tan, Z., Zhan, Z., Tan, X., Chen, Q., 2017. Characteristic of microplastics in the atmospheric fallout from Dongguan city, China: preliminary research and first evidence. Environ. Sci. Pollut. Res. 24 (32), 24928–24935. http://dx.doi.org/10.1007/s11356-017-0116-x.

Chen, G., Fu, Z., Yang, H., Wang, J., 2020. An overview of analytical methods for detecting microplastics in the atmosphere. TRAC Trends Anal. Chem. 130, 115981.

Chen, Q., Shi, G., Revell, L.E., Zhang, J., Zuo, C., Wang, D., Le Ru, E.C., Wu, G., Mitrano, D.M., 2023. Long-range atmospheric transport of microplastics across the southern hemisphere. Nature Commun. 14 (1), 7898. http://dx.doi.org/10.1038/s41467-023-43695-0.

de Souza Machado, A.A., Kloas, W., Zarfl, C., Hempel, S., Rillig, M.C., 2018. Microplastics as an emerging threat to terrestrial ecosystems. Glob. Change Biol. 24 (4), 1405–1416.

Dris, R., Gasperi, J., Saad, M., Mirande, C., Tassin, B., 2016. Synthetic fibers in atmospheric fallout: a source of microplastics in the environment? Mar. Pollut. Bull. 104 (1–2), 290–293.

Eckhardt, S., Cassiani, M., Evangeliou, N., Sollum, E., Pisso, I., Stohl, A., 2017. Source–receptor matrix calculation for deposited mass with the Lagrangian particle dispersion model FLEXPART v10. 2 in backward mode. Geosci. Model Dev. 10 (12), 4605–4618.

Evangeliou, N., Grythe, H., Klimont, Z., Heyes, C., Eckhardt, S., Lopez-Aparicio, S., Stohl, A., 2020. Atmospheric transport is a major pathway of microplastics to remote regions. Nat. Commun. 11 (1), 1–11.

Evangeliou, N., Tichỳ, O., Eckhardt, S., Zwaaftink, C.G., Brahney, J., 2022. Sources and fate of atmospheric microplastics revealed from inverse and dispersion modelling: From global emissions to deposition. J. Hazard. Mater. 432, 128585.

Fan, W., Salmond, J.A., Dirks, K.N., Cabedo Sanz, P., Miskelly, G.M., Rindelaub, J.D., 2022. Evidence and mass quantification of atmospheric microplastics in a coastal New Zealand city. Environ. Sci. Technol..

González-Pleiter, M., Lacerot, G., Edo, C., Pablo Lozoya, J., Leganés, F., Fernández-Piñas, F., Rosal, R., Teixeira-de Mello, F., 2021. A pilot study about microplastics and mesoplastics in an antarctic glacier. Cryosphere 15 (6), 2531–2539. http://dx.doi.org/10.5194/tc-15-2531-2021.

Goodman, K.E., Hare, J.T., Khamis, Z.I., Hua, T., Sang, Q.-X.A., 2021. Exposure of human lung cells to polystyrene microplastics significantly retards cell proliferation and triggers morphological changes. Chem. Res. Toxicol..

Grythe, H., Kristiansen, N.I., Groot Zwaaftink, C.D., Eckhardt, S., Ström, J., Tunved, P., Krejci, R., Stohl, A., 2017. A new aerosol wet removal scheme for the Lagrangian particle model FLEXPART v10. Geosci. Model Dev. 10 (4), 1447–1466.

Hamilton, B.M., Bourdages, M.P., Geoffroy, C., Vermaire, J.C., Mallory, M.L., Rochman, C.M., Provencher, J.F., 2021. Microplastics around an arctic seabird colony: Particle community composition varies across environmental matrices. Sci. Total Environ. 773, 145536.

Hersbach, H., Bell, B., Berrisford, P., Hirahara, S., Horányi, A., Muñoz-Sabater, J., Nicolas, J., Peubey, C., Radu, R., Schepers, D., Simmons, A., Soci, C., Abdalla, S., Abellan, X., Balsamo, G., Bechtold, P., Biavati, G., Bidlot, J., Bonavita, M., De Chiara, G., Dahlgren, P., Dee, D., Diamantakis, M., Dragani, R., Flemming, J., Forbes, R., Fuentes, M., Geer, A., Haimberger, L., Healy, S., Hogan, R.J., Hólm, E., Janisková, M., Keeley, S., Laloyaux, P., Lopez, P., Lupu, C., Radnoti, G., de Rosnay, P., Rozum, I., Vamborg, F., Villaume, S., Thépaut, J.-N., 2020. The ERA5 global reanalysis. Q. J. R. Meteorol. Soc. 146 (730), 1999–2049. http://dx.doi.org/10.1002/qj.3803.

Huang, Y., He, T., Yan, M., Yang, L., Gong, H., Wang, W., Qing, X., Wang, J., 2021. Atmospheric transport and deposition of microplastics in a subtropical urban environment. J. Hazard. Mater. 416, 126168.

Jia, Q., Duan, Y., Han, X., Sun, X., Munyaneza, J., Ma, J., Xiu, G., 2022. Atmospheric deposition of microplastics in the megalopolis (Shanghai) during rainy season: Characteristics, influence factors, and source. Sci. Total Environ. 847, 157609.

Kernchen, S., Löder, M.G., Fischer, F., Fischer, D., Moses, S.R., Georgi, C., Nölscher, A.C., Held, A., Laforsch, C., 2022a. Airborne microplastic concentrations and deposition across the Weser River catchment. Sci. Total Environ. 818, 151812.

Kernchen, S., Schmalz, H., Löder, M.G., Georgi, C., Einhorn, A., Greiner, A., Nölscher, A.C., Laforsch, C., Held, A., 2022b. Wet and dry deposition flux measurements of atmospheric microplastic particles in central Germany.

Klein, M., Fischer, E.K., 2019. Microplastic abundance in atmospheric deposition within the Metropolitan area of Hamburg, Germany. Sci. Total Environ. 685, 96–103. http://dx.doi.org/10.1016/j.scitotenv.2019.05.405.

Knobloch, E., Ruffell, H., Aves, A., Pantos, O., Gaw, S., Revell, L.E., 2021. Comparison of deposition sampling methods to collect airborne microplastics in Christchurch, New Zealand. Water Air Soil Pollut. 232 (4), 133. http://dx.doi.org/10.1007/s11270-021-05080-9.

Levermore, J.M., Smith, T.E., Kelly, F.J., Wright, S.L., 2020. Detection of microplastics in ambient particulate matter using Raman spectral imaging and chemometric analysis. Anal. Chem. 92 (13), 8732–8740.

Li, J., Zhang, J., Ren, S., Huang, D., Liu, F., Li, Z., Zhang, H., Zhao, M., Cao, Y., Mofolo, S., et al., 2023. Atmospheric deposition of microplastics in a rural region of north China plain. Sci. Total Environ. 877, 162947.

Liu, Z., Bai, Y., Ma, T., Liu, X., Wei, H., Meng, H., Fu, Y., Ma, Z., Zhang, L., Zhao, J., 2022. Distribution and possible sources of atmospheric microplastic deposition in a valley basin city (Lanzhou, China). Ecotoxicol. Environ. Saf. 233, 113353.

Liu, K., Wu, T., Wang, X., Song, Z., Zong, C., Wei, N., Li, D., 2019. Consistent transport of terrestrial microplastics to the ocean through atmosphere. Environ. Sci. Technol. 53 (18), 10612–10619.

Macara, G.R., 2016. The climate and weather of canterbury.

Marina-Montes, C., Pérez-Arribas, L.V., Anzano, J., de Vallejuelo, S.F.-O., Aramendia, J., Gómez-Nubla, L., de Diego, A., Madariaga, J.M., Cáceres, J.O., 2022. Characterization of atmospheric aerosols in the antarctic region using Raman spectroscopy and scanning electron microscopy. Spectrochim. Acta A 266, 120452.

Mbachu, O., Jenkins, G., Pratt, C., Kaparaju, P., 2020. A new contaminant superhighway? A review of sources, measurement techniques and fate of atmospheric microplastics. Water Air Soil Pollut. 231, 1–27.

McGowan, H.A., Kamber, B., McTainsh, G.H., Marx, S.K., 2005. High resolution provenancing of long travelled dust deposited on the southern Alps, New Zealand. Geomorphology 69 (1–4), 208–221.

Morét-Ferguson, S., Law, K.L., Proskurowski, G., Murphy, E.K., Peacock, E.E., Reddy, C.M., 2010. The size, mass, and composition of plastic debris in the western north Atlantic ocean. Mar. Pollut. Bull. 60 (10), 1873–1878.

Osborne, S., Johnson, B., Haywood, J., Baran, A., Harrison, M., McConnell, C., 2008. Physical and optical properties of mineral dust aerosol during the dust and biomass-burning experiment. J. Geophys. Res.: Atmos. 113 (D23).

Pisso, I., Sollum, E., Grythe, H., Kristiansen, N.I., Cassiani, M., Eckhardt, S., Arnold, D., Morton, D., Thompson, R.L., Groot Zwaaftink, C.D., et al., 2019. The Lagrangian particle dispersion model FLEXPART version 10.4. Geosci. Model Dev. 12 (12), 4955–4997.

Prata, J.C., 2018. Airborne microplastics: consequences to human health? Environ. Pollut. 234, 115–126.

Primpke, S., Wirth, M., Lorenz, C., Gerdts, G., 2018. Reference database design for the automated analysis of microplastic samples based on Fourier transform infrared (FTIR) spectroscopy. Anal. Bioanal. Chem. 410 (21), 5131–5141.

Purwiyanto, A.I.S., Prartono, T., Riani, E., Naulita, Y., Cordova, M.R., Koropitan, A.F., 2022. The deposition of atmospheric microplastics in Jakarta-Indonesia: The coastal urban area. Mar. Pollut. Bull. 174, 113195.

Revell, L.E., Kuma, P., Le Ru, E.C., Somerville, W.R.C., Gaw, S., 2021. Direct radiative effects of airborne microplastics. Nature 598 (7881), 462–467. http://dx.doi.org/10.1038/s41586-021-03864-x.

Roblin, B., Ryan, M., Vreugdenhil, A., Aherne, J., 2020. Ambient atmospheric deposition of anthropogenic microfibers and microplastics on the western periphery of Europe (Ireland). Environ. Sci. Technol. 54 (18), 11100–11108.

Seibert, P., Frank, A., 2004. Source-receptor matrix calculation with a Lagrangian particle dispersion model in backward mode. Atmos. Chem. Phys. 4 (1), 51–63. http://dx.doi.org/10.5194/acp-4-51-2004.

Sinha, V., Patel, M.R., Patel, J.V., 2010. PET waste management by chemical recycling: a review. J. Polym. Environ. 18 (1), 8–25.

Stanton, T., Johnson, M., Nathanail, P., MacNaughtan, W., Gomes, R.L., 2019. Freshwater and airborne textile fibre populations are dominated by 'natural', not microplastic, fibres. Sci. Total Environ. 666, 377–389.

Statistics New Zealand, 2018. 2018 Census: MacKenzie district. https://www.stats.govt.nz/tools/2018-census-place-summaries/mackenzie-district.

Strady, E., Kieu-Le, T.-C., Tran, Q.-V., Thuong, Q.-T., et al., 2021. Microplastic in atmospheric fallouts of a developing southeast Asian megacity under tropical climate. Chemosphere 272, 129874.

Szewc, K., Graca, B., Dołęga, A., 2021. Atmospheric deposition of microplastics in the coastal zone: Characteristics and relationship with meteorological factors. Sci. Total Environ. 761, 143272.

Tatsii, D., Bucci, S., Bhowmick, T., Guettler, J., Bakels, L., Bagheri, G., Stohl, A., 2023. Shape matters: long-range transport of microplastic fibers in the atmosphere. preprint.

Wright, S.L., Ulke, J., Font, A., Chan, K.L.A., Kelly, F.J., 2020. Atmospheric microplastic deposition in an urban environment and an evaluation of transport. Environ. Int. 136, 105411.

Xiao, S., Cui, Y., Brahney, J., Mahowald, N., Li, Q., 2023. Long-distance atmospheric transport of microplastic fibers depends on their shapes.

Yang, S., Zhang, T., Gan, Y., Lu, X., Chen, H., Chen, J., Yang, X., Wang, X., 2022. Constraining microplastic particle emission flux from the ocean. Environ. Sci. Technol. Lett. 9 (6), 513–519.

Yao, Y., Glamoclija, M., Murphy, A., Gao, Y., 2022. Characterization of microplastics in indoor and ambient air in northern New Jersey. Environ. Res. 207, 112142.

Yasunari, T.J., Koster, R.D., Lau, K.-M., Aoki, T., Sud, Y.C., Yamazaki, T., Motoyoshi, H., Kodama, Y., 2011. Influence of dust and black carbon on the snow albedo in the NASA goddard earth observing system version 5 land surface model. J. Geophys. Res.: Atmos. 116 (D2).

Yuan, Z., Pei, C., Li, H., Lin, L., Liu, S., Hou, R., Liao, R., Xu, X., 2023. Atmospheric microplastics at a southern China metropolis: Occurrence, deposition flux, exposure risk and washout effect of rainfall. Sci. Total Environ. 869, 161839.

Zhang, Y., Kang, S., Allen, S., Allen, D., Gao, T., Sillanpää, M., 2020. Atmospheric microplastics: A review on current status and perspectives. Earth-Sci. Rev. 103118.